




Clinicopathological and molecular correlations in traditional serrated adenoma

Shigeki Sekine^{1,2}  · Satoshi Yamashita³ · Masayoshi Yamada⁴ · Taiki Hashimoto¹ · Reiko Ogawa² · Hiroshi Yoshida¹ · Hirokazu Taniguchi¹ · Motohiro Kojima⁵ · Toshikazu Ushijima³ · Yutaka Saito⁴

Received: 26 June 2019 / Accepted: 22 January 2020 / Published online: 12 February 2020
© Japanese Society of Gastroenterology 2020

Abstract

Background Traditional serrated adenoma (TSA) is the least common type of colorectal serrated polyp, which exhibits considerable morphological and molecular diversity.

Methods We examined the spectra of alterations in MAPK and WNT pathway genes and their relationship with clinicopathological features in 128 TSAs.

Results Sequencing analyses identified *BRAF* V600E, *BRAF* non-V600E, *KRAS*, and *NRAS* mutations in 77, 3, 45, and 1 lesion, respectively. Collectively, 124 lesions (97%) had mutations in MAPK pathway genes. Alterations in WNT pathway genes were identified in 107 lesions (84%), including *RSPO* fusions/overexpression, *RNF43* mutations, *ZNRF3* mutations, *APC* mutations, and *CTNNB1* mutations in 47, 45, 2, 13, and 2 lesions, respectively. Ten lesions (8%) harbored *GNAS* mutations. There was significant interdependence between the altered MAPK and WNT

pathway genes. *RSPO* fusions/overexpression was significantly associated with *KRAS* mutations (31/47, 66%), whereas most *RNF43* mutations coexisted with the *BRAF* V600E mutation (40/45, 89%). Histologically, extensive slit-like serration was more common in lesions with the *BRAF* V600E mutation (71%) and those with *RNF43* mutations (87%). Prominent ectopic crypt formation was more prevalent in lesions with *RSPO* fusions/overexpression (58%) and those with *GNAS* mutations (100%).

Conclusions Our observations indicate that TSAs mostly harbor various combinations of concurrent WNT and MAPK gene alterations. The associations between genetic and morphological features suggest that the histological diversity of TSA reflects the underlying molecular heterogeneity.

Keywords Traditional serrated adenoma · WNT pathway · MAPK pathway

Electronic supplementary material The online version of this article (<https://doi.org/10.1007/s00535-020-01673-z>) contains supplementary material, which is available to authorized users.

✉ Shigeki Sekine
ssekine@ncc.go.jp

- ¹ Division of Pathology and Clinical Laboratories, National Cancer Center Hospital, 5-1-1, Tsukiji, Chuo-ku, Tokyo 104-0045, Japan
- ² Division of Molecular Pathology, National Cancer Center Research Institute, Tokyo, Japan
- ³ Division of Epigenomics, National Cancer Center Research Institute, Tokyo, Japan
- ⁴ Endoscopy Division, National Cancer Center Hospital, Tokyo, Japan
- ⁵ Division of Pathology, Research Center for Innovative Oncology, National Cancer Center, Kashiwa, Chiba, Japan

Introduction

Recent studies have suggested that approximately 20–30% of colorectal cancers are derived from serrated lesions [1, 2]. Serrated lesions include hyperplastic polyps, sessile serrated adenoma/polyps (SSA/Ps), and traditional serrated adenomas (TSAs) [3]. Among these, TSA is the least common subtype and is associated with premalignant potential, along with sessile serrated adenoma/polyp [4]. The histological features of TSA include abundant eosinophilic cytoplasm, elongated nuclei, ectopic crypt formation, and slit-like serration [5–7]. It is well established that TSA represents a distinct entity and the histological diagnosis is usually straightforward. However, it is also true that TSAs exhibit significant morphological

heterogeneity. For instance, the presence of ectopic crypt formation is characteristic but not a consistent feature of TSAs [6]. Although still not widely accepted, some authors have suggested some morphological subtypes of TSAs, including mucin-rich and filiform variants [8–10].

Serrated polyps mostly harbor genetic alterations leading to MAPK pathway activation, mostly *KRAS* or *BRAF* mutations [6, 11–14]. *KRAS* mutations are common in goblet cell-rich hyperplastic polyps whereas microvesicular hyperplastic polyps and SSA/Ps frequently harbor the *BRAF* V600E mutation [15–17]. TSAs also frequently have MAPK pathway gene mutations, but unlike others, both *BRAF* and *KRAS* mutations are detected in TSAs, indicating their molecular variability [6, 11–14]. Furthermore, our previous studies showed that the majority of TSAs also harbor alterations in WNT pathway genes, including *RSPO* fusions/overexpression, *RNF43* mutations, and *APC* mutations, introducing another layer of genetic heterogeneity [18, 19].

Based on these previous observations, we postulated that the morphological variability of TSAs might reflect their molecular heterogeneity. The present study aimed to investigate the spectrum of genetic alterations in a larger series of TSAs and assessed their clinicopathological correlations.

Materials and methods

Samples

This study was approved by the Ethics Committee of the National Cancer Center, Tokyo, Japan. Tissue samples were obtained by endoscopic resection at the National Cancer Center Hospital, Tokyo, Japan, or at the National Cancer Center Hospital East, Chiba, Japan. We analyzed 128 TSAs, which were examined in our previous studies [18, 19]. Samples with insufficient quality of DNA and/or RNA for next-generation sequencing or reverse transcription PCR were excluded from the present study.

Histological analysis

All TSAs were confirmed to exhibit at least two of the following three histological features: (1) typical cytology, (2) slit-like epithelial serrations, and (3) ectopic crypt formation, with at least one feature present in > 50% of the polyps excluding the precursor component (Fig. 1a–d) [6]. The areas exhibiting typical cytology, slit-like serrations and ectopic crypt formation were semi-quantitatively evaluated as < 10%, 10–50%, or > 50% (regarded as extensive/prominent). The proportion of goblet cells/mucin-rich cells was also semiquantitatively evaluated as

< 10%, 10–50%, or > 50% (Fig. 1e, f). The presence of high-grade components and the association of hyperplastic polyp, SSA/P, and superficially serrated adenoma were determined (Figs. 1g, 2a–d). The cecum to the transverse colon was defined as the right colon and the descending colon to the sigmoid colon was defined as the left colon.

Molecular characterization

The detailed methods and part of the results of molecular analyses were described in our previous studies [18, 19]. Outlines of the analytical methods are as follows.

Sections of formalin-fixed paraffin-embedded specimens were dissected under a microscope using sterilized toothpicks to enrich for tumor content and were used for DNA and RNA extraction. In the analysis of precursor polyp-associated lesions, we subjected only TSA components to DNA and RNA extraction.

For next-generation sequencing, amplicon libraries, targeting frequently mutated regions of *APC*, *BRAF*, *CTNNB1*, *GNAS*, *KRAS*, and *NRAS*, and the entire coding regions of *RNF43* and *ZNRF3*, were prepared using the Ion AmpliSeq™ custom panel (ThermoFisher Scientific, Waltham, MA, USA). Sequencing was performed using an Ion Proton Sequencer, an Ion PI Chip, and an Ion PI Hi-Q Sequencing 200 Kit (ThermoFisher Scientific). The sequences obtained were mapped onto the human reference genome hg19, and sequence variations with variant frequencies > 10% for single-nucleotide variants and 15% for insertions/deletions were identified as candidate mutations. Synonymous mutations and common single nucleotide polymorphism, based on the Single Nucleotide Polymorphism Database build 137, were excluded. All resulting mutation candidates were confirmed using Sanger sequencing. Part of the sequencing results was previously reported [18].

The presence of overexpression and fusions of *RSPO2* and *RSPO3* was tested using quantitative PCR and the specific fusions were detected by conventional reverse transcription PCR. The results of *RSPO* fusion and overexpression analyses were described previously [19].

CpG island methylator phenotype (CIMP) status was assessed by the quantitative methylation-specific PCR using the panel of Weisenberger et al. (*NEUROG1*, *CACNA1G*, *IGF2*, *RUNX3*, and *SOC31*) [20]. Lesions were classified by the number of markers showing a percentage of the methylated reference ≥ 10 as follows: CIMP-high, ≥ 3 ; CIMP-low, 1 or 2; and CIMP-negative, no markers. Part of the methylation analysis was previously reported [18].

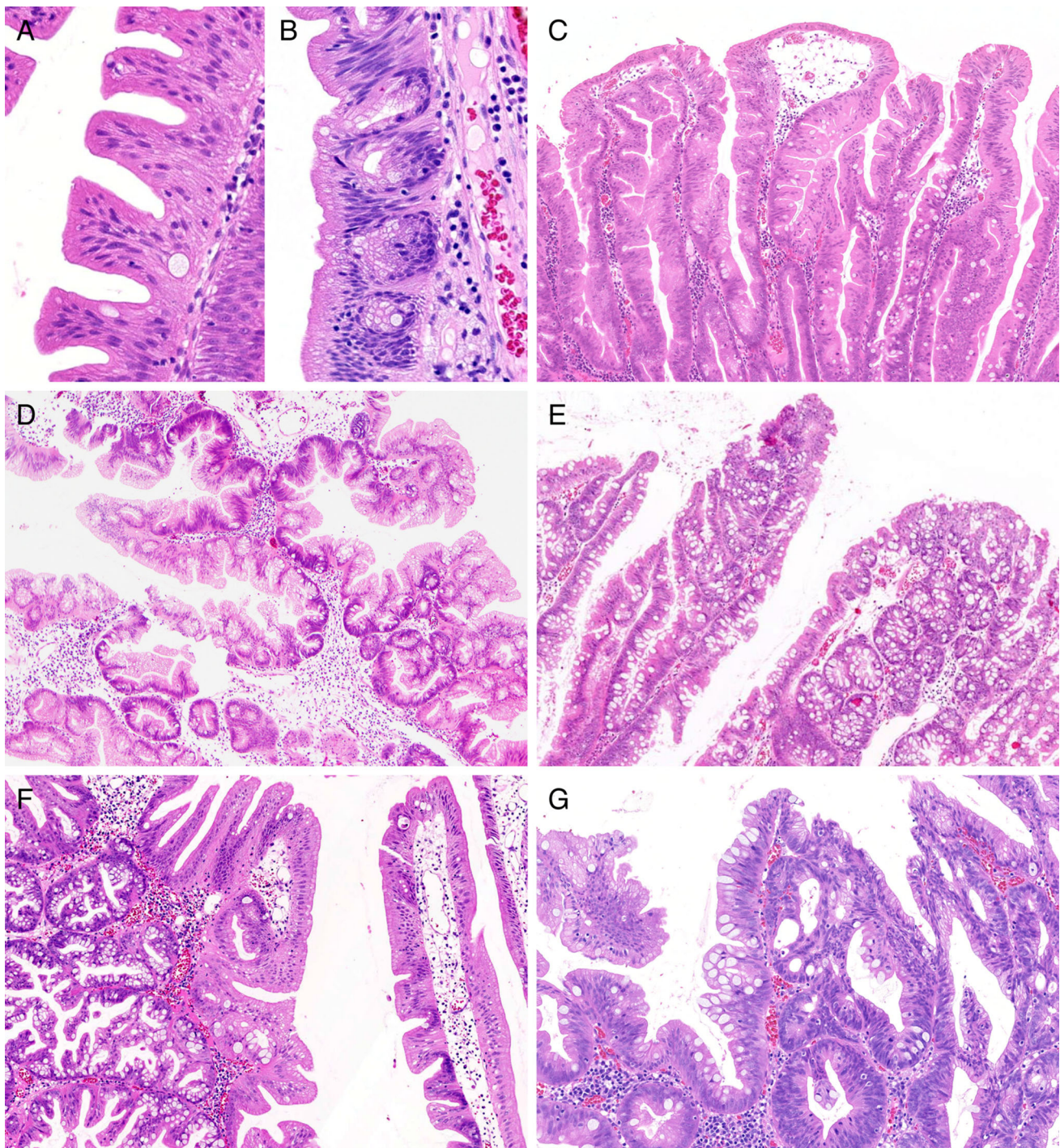


Fig. 1 Representative histology of traditional serrated adenomas. **a** Slit-like serration. Narrow slits in the epithelium exhibiting eosinophilic cytoplasm. **b** Ectopic crypt formations. Epithelial buds along the villous projection. **c** Tumor cells showing abundant

eosinophilic cytoplasm and prominent slit-like serration. **d** TSA with prominent ectopic crypt formation. **e** TSA containing numerous goblet cells. **f** TSA showing a focal goblet cell-rich area (left). **g** A lesion associated with a high-grade component (right)

Immunohistochemistry

Immunohistochemical staining for MLH1 was performed as described previously [18]. Part of the staining results was previously reported [18].

Statistical analysis

Fisher's exact test and Welch's t-test were used to analyze categorical variables and continuous variables,

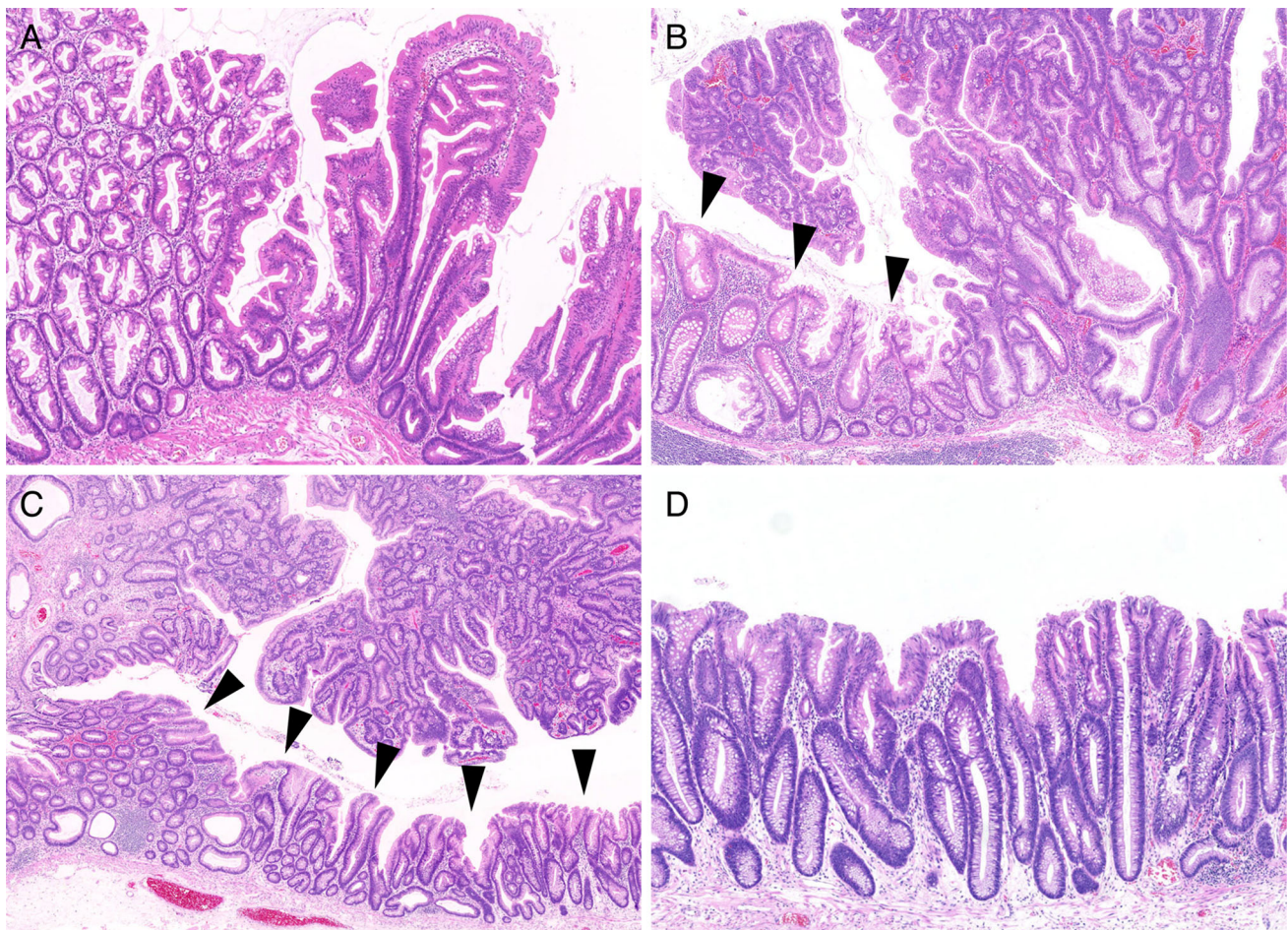


Fig. 2 Traditional serrated adenoma associated with precursor polyps. TSAs with a hyperplastic polyp (a, left) and a sessile serrated polyp (b, arrowheads), respectively. TSA with a superficially serrated

adenoma (c, arrowheads). The superficially serrated adenoma component shows adenomatous glands with mild serration confined to the superficial layer (d)

respectively. *P* values < 0.01 were considered to indicate statistical significance.

Results

The TSAs were obtained from 80 male and 48 female patients who were aged 34–85 years (median, 68 years). The distribution of the polyps was as follows: 22 lesions (17%) in the right colon, 51 (40%) in the left colon, and 55 (43%) in the rectum. They were 2–58 mm in size (median, 7 mm). A high-grade component was seen in 21 lesions (16%). The association of hyperplastic polyp, SSA/P, and superficially serrated adenoma was observed in 22 (17%), 11 (9%), and 15 lesions (12%), respectively. Typical cytology was observed in all lesions and extensive in 118 lesions (92%). Slit-like serration, ectopic crypt formation, and goblet cells were prominent (> 50% of areas or cells) in 72 (56%), 49 (38%), and 19 lesions (15%), respectively.

Twenty-four lesions (19%) showed the CIMP-high phenotype.

Next-generation sequencing followed by confirmation by Sanger sequencing identified 57 *RNF43*, 10 *ZNRF3*, 18 *APC*, 2 *CTNNB1*, 80 *BRAF*, 46 *KRAS*, 1 *NRAS*, and 10 *GNAS* mutations (Supplementary Table 1). Among the tumor suppressor genes examined, eight *RNF43*, eight *ZNRF3*, and three *APC* mutations were missense. Since the functional consequences of these missense mutations were unclear, only protein-truncating mutations have been considered as inactivating mutations hereafter. Mutations detected in *CTNNB1*, *KRAS*, *NRAS*, and *GNAS* have been previously reported in diverse tumors and regarded as oncogenic. A total of six lesions had two *RNF43*, *APC*, or *KRAS* mutations. Quantitative and conventional reverse transcription-PCR detected *PTPRK-RSPO3* fusions, an *NRIP1-RSPO2* fusion, *RSPO2* overexpression, and *RSPO3* overexpression in 42, 1, 2, and 2 lesions, respectively.

Collectively, alterations in MAPK pathway genes were identified in 124 lesions (97%; Fig. 3). *BRAF* V600E,

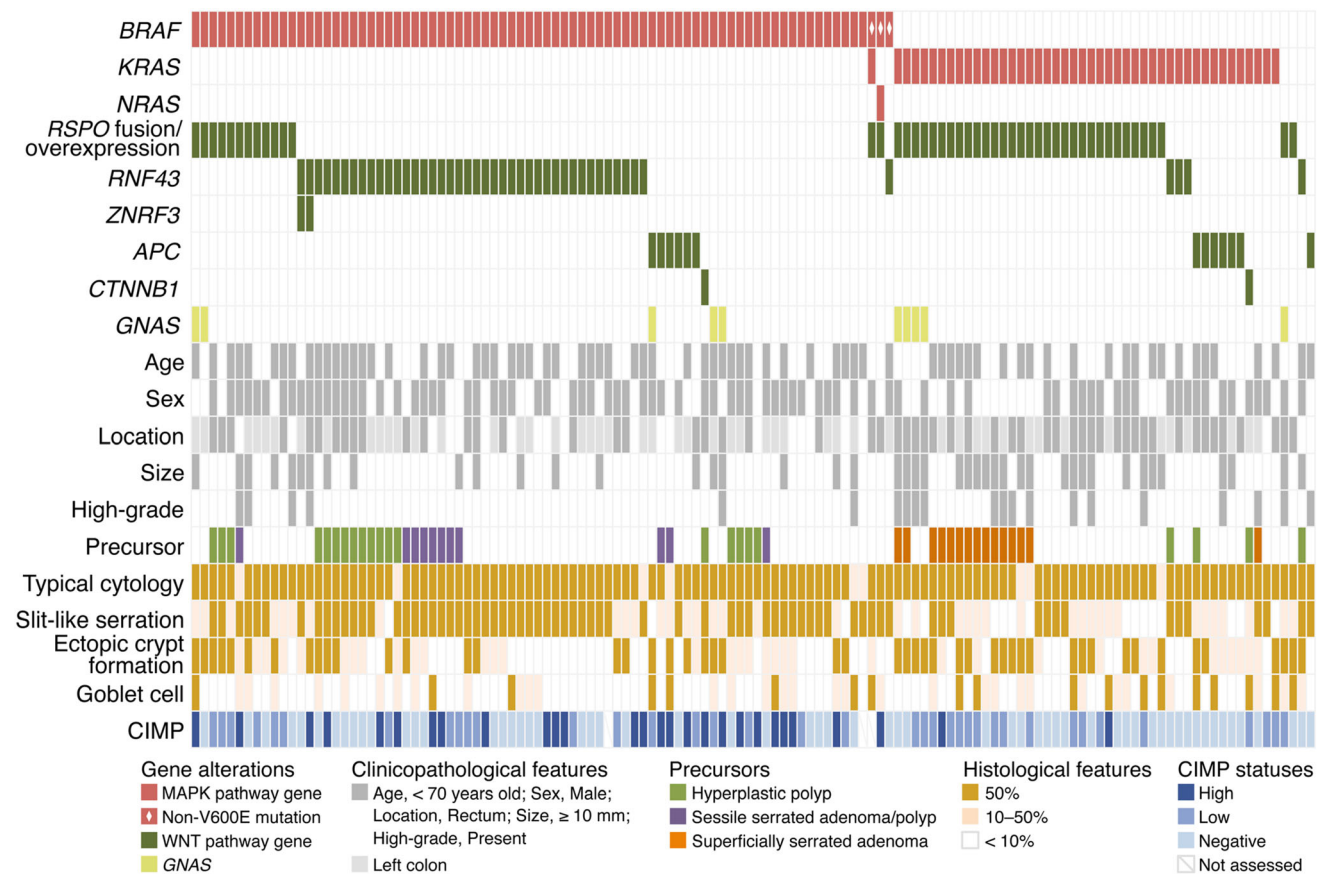


Fig. 3 Molecular and clinicopathological features of traditional serrated adenomas. Only protein-truncating mutations are indicated for *RNF43*, *ZNRF3*, and *APC* mutations

KRAS, and *NRAS* mutations were mutually exclusive to each other. In contrast, two of the three TSAs with *BRAF* non-V600E mutations also had a *KRAS* or *NRAS* mutation; therefore, lesions with the *BRAF* V600E and non-V600E mutations were analyzed as separate groups. Alterations in WNT pathway genes were detected in 107 lesions (84%). *RSPO* fusions/overexpression, *RNF43* mutations, *APC* mutations, and *CTNNB1* mutations were mutually exclusive to each other. In contrast, the two lesions with truncating *ZNRF3* mutations concurrently harbored *RNF43* mutations, consistent with their cooperative roles with *RNF43* mutations [18, 21]. Overall, 80% of TSAs possessed alterations in both WNT and MAPK pathways.

Since the numbers of lesions with *BRAF* non-V600E and those lacking MAPK gene mutations were too small for statistical analyses, we compared TSAs with the *BRAF* V600E and *KRAS* mutations for their clinicopathological characteristics (Table 1). There was significant interdependence between alterations in MAPK and WNT pathway genes. *KRAS* mutations were associated with *RSPO* fusions/overexpression (31/44, 70%). More than half of the lesions with the *BRAF* V600E mutation also harbored *RNF43* mutations (40/77, 52%); conversely, most *RNF43*

mutations coexisted with the *BRAF* V600E mutation (40/45, 89%). TSAs with the *BRAF* V600E mutations were more likely to be located in the proximal colon and less frequently had high-grade components. The association with hyperplastic polyps and SSA/Ps was common in lesions with the *BRAF* V600E mutations. As previously reported [22], superficially serrated adenoma exclusively coexisted with *KRAS*-mutated TSAs. Slit-like serration and ectopic crypt formation were more extensive in *BRAF*-mutated and *KRAS*-mutated TSAs, respectively. The CIMP-high phenotype was more common in *BRAF*-mutated TSAs.

With regard to WNT pathway gene mutations, clinicopathological features associated with *RSPO* fusions/overexpression, *RNF43* mutations, and *APC* mutations were examined (Table 2). TSAs with *RSPO* fusions/overexpression were rare in the proximal colon, and were slightly larger in size than others. The presence of a high-grade component was more frequent in TSAs with *RSPO* fusions, but was rare in TSAs with *RNF43* mutations. Hyperplastic polyps and SSA/Ps were more commonly associated with *RNF43*-mutated TSAs, whereas superficially serrated adenoma was almost exclusively associated with TSAs with

Table 1 Clinicopathological features of traditional serrated adenomas according to alterations in MAPK pathway genes

	<i>BRAF</i> V600E <i>n</i> = 77 (60%)	<i>BRAF</i> non-V600E <i>n</i> = 3 (2%)	<i>KRAS</i> <i>n</i> = 44 (34%)	No mutations <i>n</i> = 4 (3%)	<i>BRAF</i> V600E vs. <i>KRAS</i>
<i>RSPO</i> fusion/overexpression	12 (16%)	2 (67%)	31 (70%)	2 (50%)	1.7×10^{-9}
<i>RNF43</i> mutation	40 (52%)	1 (33%)	3 (7%)	1 (25%)	3.4×10^{-7}
<i>APC</i> mutation	6 (8%)	0	6 (14%)	1 (25%)	0.35
<i>CTNNB1</i> mutation	1 (1%)	0	1 (2%)	0	Not assessed
<i>GNAS</i> mutation	5 (6%)	0	4 (9%)	1 (25%)	0.72
Age, year-old, median (range)	67 (40–81)	72 (65–79)	70 (34–85)	70 (52–85)	0.76
Male/Female	53/24	2/1	23/21	2/2	0.081
Right colon/Left colon/Rectum	19/35/23	0/1/2	1/15/28	2/0/2	0.0016 ^a
Size, mm, median (range)	7 (3–58)	4 (3–5)	9.5 (2–54)	10 (4–19)	0.012
High-grade component	6 (8%)	0	13 (30%)	2 (50%)	0.0022
Hyperplastic polyp or SSA/P	18/11 (38%)	0/0	3/0 (7%)	1/0 (25%)	0.00019
SuSA component	0	0	15 (34%)	0	4.3×10^{-8}
Slit-like serration ^b	55/19/3	3/0/0	12/18/14	2/2/0	3.5×10^{-6c}
Ectopic crypt formation ^b	25/22/30	0/1/2	21/12/11	3/0/1	0.12 ^c
Goblet cells ^b	7/19/51	1/1/1	10/10/24	1/2/1	0.056 ^c
CIMP high/low/negative ^d	25/19/31	1/0/1	2/17/25	0/1/3	0.00051 ^c

SSA/P, sessile serrated adenoma/polyp; SuSA, superficially serrated adenoma

Two TSAs with *BRAF* non-V600E mutations also had a *KRAS* or *NRAS* mutation

^aRight colon vs. left colon and rectum

^b> 50/50–10/< 10% areas

^c> 50% vs. ≤ 50%

^dNot assessed for three cases

^eCIMP-high vs. -low/negative

RSPO fusions/overexpression. Slit-like serration and ectopic crypt formation were more extensive in TSAs with *RNF43* mutations and *RSPO* fusions/overexpression, respectively.

GNAS mutations were significantly associated with older age, the presence of high-grade components, less slit-like serration, and extensive ectopic crypt formation (Table 3).

MLH1 expression was retained in all lesions, except for one lesion in which a section for immunohistochemical staining was unavailable (Supplementary Table 1).

Discussion

Our analysis identified concurrent alterations in MAPK and WNT pathway genes in four-fifths of TSAs. The frequency of MAPK pathway-related mutations was higher than those reported in most previous studies, which is partly because these studies focused on mutations in codon 600 of *BRAF* and codon 12 and 13 of *KRAS* [6, 11–14]. Our analysis identified three *BRAF* and seven *KRAS* mutations outside these most commonly mutated residues and one *NRAS*

mutation. Most MAPK pathway gene alterations were mutually exclusive of each other, but two of the three TSAs with a *BRAF* non-V600E mutation concurrently harbored a *KRAS* or *NRAS* mutation. This finding is similar to our previous observation on SSA/P, demonstrating that all three lesions with *BRAF* non-V600E mutations also had a *KRAS* or *NRAS* mutation [17], and is consistent with the fact that many *BRAF* non-V600E mutations are loss-of-function mutations but enhance MAPK signaling in cooperation with active RAS [23, 24].

We used the Weisenberger panel to determine the CIMP status in the present study [20]. Although this panel was originally designed to correlate with the presence of *BRAF* mutations in colorectal cancers, recent studies have shown the association between the *BRAF* V600E mutation and the CIMP-high phenotype also in the precursor lesions using this panel [6, 14]. Consistently, the CIMP-high phenotype was more common in lesions with the *BRAF* V600E mutation also in the present study.

Mutations related to the WNT pathway are virtually ubiquitous in colorectal cancers and are thought to be the initial genetic alterations in the conventional pathway of tumorigenesis [25, 26]. In the serrated pathway of

Table 2 Clinicopathological features of traditional serrated adenomas according to alterations in WNT pathway genes

	<i>RSPO</i> <i>n</i> = 47 (37%)	<i>RNF43</i> <i>n</i> = 45 (35%)	<i>APC</i> <i>n</i> = 13 (10%)	<i>CTNNB1</i> <i>n</i> = 2 (2%)	No mutations <i>n</i> = 21 (16%)	<i>RSPO</i> vs. others	<i>RNF43</i> vs. others	<i>APC</i> vs. others
<i>GNAS</i> mutation	7 (15%)	0	1 (8%)	0	2 (10%)	0.037	0.014	1.0
Age, year-old, median (range)	69 (37–85)	67 (41–81)	70 (34–76)	58, 70	67 (51–85)	0.74	0.71	0.94
Male/female	23/24	33/12	7/6	2/0	15/6	0.023	0.085	0.55
Right colon/left colon/rectum ^a	2/16/29	10/20/15	3/4/6	0/1/1	7/10/4	0.0030	0.33	0.70
Size, mm, median (range)	11 (3–54)	6 (3–19)	9 (4–38)	5, 7	7 (2–58)	0.0046	0.00011	0.83
High-grade component	15 (32%)	1 (2%)	2 (15%)	0	3 (14%)	0.00049	0.0020	1.0
Hyperplastic polyp or SSA/P	3/1 (9%)	12/7 (42%)	1/2 (23%)	2/0 (100%)	4/1 (24%)	0.00065	0.0028	1.0
SuSA component	14 (30%)	0	0	0	1 (5%)	2.2 × 10 ⁻⁶	0.0026	0.23
Slit-like serration ^b	15/21/11	39/5/1	2/8/3	1/1/0	15/4/2	3.8 × 10 ^{-5c}	2.4 × 10 ^{-7c}	0.0023 ^c
Ectopic crypt formation ^b	27/11/9	11/10/24	5/5/3	1/1/0	5/8/8	0.00080 ^c	0.022 ^c	1.0 ^c
Goblet cells ^b	9/13/25	2/11/32	4/0/9	1/0/1	3/8/10	0.31 ^c	0.018 ^c	0.10 ^c
CIMP high/low/negative ^d	5/21/20	12/7/25	3/2/8	1/1/0	7/6/7	0.025 ^e	0.37 ^e	1.0 ^e

RSPO, *RSPO* fusions/overexpression; *SSA/P*, sessile serrated adenoma/polyp; *SuSA*, superficially serrated adenoma

^aRight colon vs. left colon and rectum

^b> 50%/50–10/< 10% areas

^c> 50% vs. ≤ 50%

^dNot assessed for three cases

^eCIMP-high vs. -low/negative

Table 3 Clinicopathological features of traditional serrated adenomas according to *GNAS* mutation status

	<i>GNAS</i> -mutated <i>n</i> = 10 (8%)	<i>GNAS</i> wild-type <i>n</i> = 118 (92%)	<i>P</i> value
Age, year-old, median (range)	71 (66–85)	67 (34–85)	0.0069
Male/female	5/5	75/43	0.50
Right colon/left colon/rectum ^a	0/4/6	22/47/49	0.21
Size, mm, median (range)	23.5 (4–58)	7 (2–49)	0.021
High-grade component	6 (60%)	15 (13%)	0.0013
Hyperplastic polyp or SSA/P	0/0	22/11 (28%)	0.063
SuSA component	2 (20%)	13 (11%)	0.61
Slit-like serration ^b	0/7/3	72/32/14	1.6×10^{-4c}
Ectopic crypt formation ^b	10/0/0	39/35/44	3.6×10^{-5c}
Goblet cells ^b	2/2/6	17/30/71	0.64 ^c
CIMP high/low/negative ^d	2/5/3	26/32/57	1.0 ^e

SSA/P, sessile serrated adenoma/polyp; SuSA, superficially serrated adenoma

^aRight colon vs. left colon and rectum^b> 50%/50–10%/< 10% areas^c> 50% vs. ≤ 50%^dNot assessed for three cases^eCIMP-high vs. -low/negative

tumorigenesis, MAPK pathway gene alterations are the initial event and alterations in WNT pathway genes are acquired during the transition from non-dysplastic to dysplastic lesions [27–29]. Consistently, alterations in WNT pathway genes were detected in the majority of TSAs; however, the mutation spectrum was different from that of conventional adenomas. Most conventional adenomas possess inactivating *APC* mutations and less frequently, *CTNGB1* mutations [18, 30, 31]. In contrast, *RSPO* fusions/overexpression and *RNF43* mutations were predominant mutations in TSAs [18, 19]. Indeed, similar to the *BRAF* V600E mutation, these two genetic alterations are specific to serrated lesions [18, 32]. Interestingly, *RSPO* fusions/overexpression was significantly associated with *KRAS* mutations and most *RNF43* mutations coexisted with the *BRAF* V600E mutation, indicating the interdependence between MAPK and WNT pathway gene mutations.

GNAS mutations were identified in 8% of the lesions, a frequency similar to those reported by other studies [14, 33]. While the number of *GNAS*-mutated lesions was limited, they correlated with several clinicopathological features, including the presence of extensive ectopic crypt formation. On the other hand, there was no apparent association between *GNAS* and other mutations.

MLH1 expression was retained in all TSAs examined, in agreement with previous studies [6, 11]. This observation suggests that mismatch repair deficiency does not play a role in the development of TSA unlike tumorigenesis via SSA/P with dysplasia [27, 34, 35].

Slit-like serration and ectopic crypt formation are characteristic histological features of TSAs [5–7].

Although both these features are observed in the majority of TSAs and commonly coexist, their extent varies among lesions [6]. Our results showed the correlations between genetic alterations and these histological observations. Extensive slit-like serration was associated with the *BRAF* V600E mutation and *RNF43* mutations whereas it was less common in lesions with *RSPO* fusions/overexpression and *APC* mutations. Prominent ectopic crypt formation was frequent in lesions with *RSPO* fusions/overexpression and *GNAS* mutations. The correlations between morphology and genetic alterations suggest that although each of the alterations in MAPK and WNT pathway genes activates common signaling pathways, they have different biological activities. However, lesions with different genotypes exhibited overlapping histological features, supporting the validity to regard TSA as a single entity despite its genetic diversity.

Recent studies have suggested that the mucin-rich variant of TSA, which is defined as lesions containing ≥ 50% goblet cells, should be regarded as a distinct histological subtype [9, 10]. The prevalence of mucin-rich TSA was reported to be 15–28%, which is consistent with our findings. However, there was considerable variability in the number of goblet cells among the polyps, and the distribution of goblet cells showed notable heterogeneity within the respective lesions. Therefore, although it is true that some TSAs are rich in goblet cells, we are hesitant to regard them as a histologically distinct variant. A previous study reported that mucin-rich TSAs were more likely to have *BRAF* mutations [10]; however, this finding was not reproduced in our analysis.

The presence of a high-grade component was more frequent in lesions with *KRAS* mutations, *RSPO* fusions/overexpression, and *GNAS* mutation. This implies that TSAs with these genetic alterations may have a higher risk of malignant progression, but this hypothesis requires confirmation by analysis of lesions associated with adenocarcinoma. Consistent with our finding, the correlation between *KRAS* mutations and higher-grade dysplasia was also described in a previously study [12]. In contrast, high-grade dysplasia was rare among lesions with *BRAF* and/or *RNF43* mutations, including those associated with SSA/P. It is generally believed that once SSA/Ps acquire dysplasia, they quickly progress to adenocarcinoma [34]; however, considering the rarity of high-grade dysplasia in SSA/P-associated TSA, it may not always be the case.

The present study demonstrated the common coexistence of mutations leading to WNT and MAPK pathway activation in TSAs. Importantly, various genetic alterations are involved in the activation of the respective pathways and each genetic alteration is significantly associated with different clinical and morphological features. These findings suggest that the histological variability of TSAs reflects their mutational diversity.

Acknowledgements This work was supported by JSPS KAKENHI Grant numbers 17K08711 and 18K07925. We thank Ms. Sachiko Miura, Ms. Toshiko Sakaguchi, Ms. Chizu Kina, and Yuka Nakamura for their skillful technical assistance.

Conflict of interest The authors declare no conflicts of interest.

References

- Bettington M, Walker N, Clouston A, et al. The serrated pathway to colorectal carcinoma: current concepts and challenges. *Histopathology*. 2013;62:367–86.
- Rosty C, Hewett DG, Brown IS, et al. Serrated polyps of the large intestine: current understanding of diagnosis, pathogenesis, and clinical management. *J Gastroenterol*. 2013;48:287–302.
- Snover DC, Ahnen DJ, Burt RW, et al. Serrated polyps of the colon and rectum and serrated polyposis. In: Bosman FT, Carneiro F, Hruban RH, Theise ND, editors. *WHO classification of tumours of the digestive system*. Lyon: IARC; 2010. p. 160–165.
- Rex DK, Ahnen DJ, Baron JA, et al. Serrated lesions of the colorectum: review and recommendations from an expert panel. *Am J Gastroenterol*. 2012;107:1315–29 (**quiz 4, 30**).
- Torlakovic EE, Gomez JD, Driman DK, et al. Sessile serrated adenoma (SSA) vs. traditional serrated adenoma (TSA). *Am J Surg Pathol*. 2008;32:21–9.
- Bettington ML, Walker NI, Rosty C, et al. A clinicopathological and molecular analysis of 200 traditional serrated adenomas. *Mod Pathol*. 2015;28:414–27.
- Chetty R. Traditional serrated adenoma (TSA): morphological questions, queries and quandaries. *J Clin Pathol*. 2016;69:6–11.
- Yantiss RK, Oh KY, Chen YT, et al. Filiform serrated adenomas: a clinicopathologic and immunophenotypic study of 18 cases. *Am J Surg Pathol*. 2007;31:1238–45.
- Kalimuthu SN, Serra S, Hafezi-Bakhtiari S, et al. Mucin-rich variant of traditional serrated adenoma: a distinct morphological variant. *Histopathology*. 2017;71:208–16.
- Hiroimoto T, Murakami T, Akazawa Y, et al. Immunohistochemical and genetic characteristics of a colorectal mucin-rich variant of traditional serrated adenoma. *Histopathology*. 2018;73:444–53.
- O'Brien MJ, Yang S, Mack C, et al. Comparison of microsatellite instability, CpG island methylation phenotype, BRAF and KRAS status in serrated polyps and traditional adenomas indicates separate pathways to distinct colorectal carcinoma end points. *Am J Surg Pathol*. 2006;30:1491–501.
- Kim KM, Lee EJ, Kim YH, et al. KRAS mutations in traditional serrated adenomas from Korea herald an aggressive phenotype. *Am J Surg Pathol*. 2010;34:667–75.
- Tsai JH, Liao JY, Lin YL, et al. Traditional serrated adenoma has two pathways of neoplastic progression that are distinct from the sessile serrated pathway of colorectal carcinogenesis. *Mod Pathol*. 2014;27:1375–85.
- Wiland HOT, Shadrach B, Allende D, et al. Morphologic and molecular characterization of traditional serrated adenomas of the distal colon and rectum. *Am J Surg Pathol*. 2014;38:1290–7.
- O'Brien MJ, Yang S, Clebanoff JL, et al. Hyperplastic (serrated) polyps of the colorectum: relationship of CpG island methylator phenotype and K-ras mutation to location and histologic subtype. *Am J Surg Pathol*. 2004;28:423–34.
- Spring KJ, Zhao ZZ, Karamatic R, et al. High prevalence of sessile serrated adenomas with BRAF mutations: a prospective study of patients undergoing colonoscopy. *Gastroenterology*. 2006;131:1400–7.
- Cho H, Hashimoto T, Yoshida H, et al. Reappraisal of the genetic heterogeneity of sessile serrated adenoma/polyp. *Histopathology*. 2018;73:672–80.
- Sekine S, Yamashita S, Tanabe T, et al. Frequent PTPRK-RSPO3 fusions and RNF43 mutations in colorectal traditional serrated adenoma. *J Pathol*. 2016;239:133–8.
- Sekine S, Ogawa R, Hashimoto T, et al. Comprehensive characterization of RSPO fusions in colorectal traditional serrated adenomas. *Histopathology*. 2017;71:601–9.
- Weisenberger DJ, Siegmund KD, Campan M, et al. CpG island methylator phenotype underlies sporadic microsatellite instability and is tightly associated with BRAF mutation in colorectal cancer. *Nat Genet*. 2006;38:787–93.
- de Lau W, Peng WC, Gros P, et al. The R-spondin/Lgr5/Rnf43 module: regulator of Wnt signal strength. *Genes Dev*. 2014;28:305–16.
- Hashimoto T, Tanaka Y, Ogawa R, et al. Superficially serrated adenoma: a proposal for a novel subtype of colorectal serrated lesion. *Mod Pathol*. 2018;31:1588–98.
- Heidorn SJ, Milagre C, Whittaker S, et al. Kinase-dead BRAF and oncogenic RAS cooperate to drive tumor progression through CRAF. *Cell*. 2010;140:209–21.
- Nieto P, Ambrogio C, Esteban-Burgos L, et al. A Braf kinase-inactive mutant induces lung adenocarcinoma. *Nature*. 2017;548:239–43.
- Fearon ER, Vogelstein B. A genetic model for colorectal tumorigenesis. *Cell*. 1990;61:759–67 (**Epub 1990/06/01**).
- Cancer Genome Atlas N. Comprehensive molecular characterization of human colon and rectal cancer. *Nature*. 2012;487:330–7.
- Hashimoto T, Yamashita S, Yoshida H, et al. WNT pathway gene mutations are associated with the presence of dysplasia in colorectal sessile serrated adenoma/polyps. *Am J Surg Pathol*. 2017;41:1188–97.

28. Borowsky J, Dumenil T, Bettington M, et al. The role of APC in WNT pathway activation in serrated neoplasia. *Mod Pathol.* 2018;31:495–504.
29. Hashimoto T, Ogawa R, Yoshida H, et al. Acquisition of WNT pathway gene alterations coincides with the transition from precursor polyps to traditional serrated adenomas. *Am J Surg Pathol.* 2019;43:132–9.
30. Powell SM, Zilz N, Beazer-Barclay Y, et al. APC mutations occur early during colorectal tumorigenesis. *Nature.* 1992;359:235–7 (**Epub 1992/09/17**).
31. Borrás E, San Lucas FA, Chang K, et al. Genomic landscape of colorectal mucosa and adenomas. *Cancer Prev Res (Phila).* 2016;9:417–27.
32. Tsai JH, Liao JY, Yuan CT, et al. RNF43 is an early and specific mutated gene in the serrated pathway, with increased frequency in traditional serrated adenoma and its associated malignancy. *Am J Surg Pathol.* 2016;40:1352–9.
33. Liu C, McKeone DM, Walker NI, et al. GNAS mutations are present in colorectal traditional serrated adenomas, serrated tubulovillous adenomas and serrated adenocarcinomas with adverse prognostic features. *Histopathology.* 2017;70:1079–88.
34. Bettington M, Walker N, Rosty C, et al. Clinicopathological and molecular features of sessile serrated adenomas with dysplasia or carcinoma. *Gut.* 2017;66:97–106.
35. Liu C, Walker NI, Leggett BA, et al. Sessile serrated adenomas with dysplasia: morphological patterns and correlations with MLH1 immunohistochemistry. *Mod Pathol.* 2017;30:1728–38.

Publisher's Note Springer Nature remains neutral with regard to jurisdictional claims in published maps and institutional affiliations.